Proceedings of the 4th WSEAS Int. Conf. on HEAT TRANSFER, THERMAL ENGINEERING and ENVIRONMENT, Elounda, Greece, August 21-23, 2006 (pp357-362)

Double Diffusive Convection from a Permeable Horizontal Cylinder of Elliptic Cross Section in a Saturated Porous Medium

CHING-YANG CHENG
Department of Mechanical Engineering
Southern Taiwan University of Technology
1, Nantai Street, Yungkang 710
TAIWAN

Abstract: - The double diffusive convection near a permeable horizontal cylinder of elliptic cross section with uniform wall temperature and concentration in a fluid-saturated porous medium are numerically studied. A coordinate transformation is employed to transform the governing equations into nondimensional nonsimilar boundary layer equations. The obtained boundary layer equations are then solved by the cubic spline collocation method. The influence of the transpiration parameter and the eccentricity on the heat and mass transfer characteristics near a permeable horizontal cylinder of elliptic cross section in a fluid-saturated porous medium is examined as the major axis of the elliptic cylinder is vertical (slender orientation) and horizontal (blunt orientation). Increasing the transpiration parameter tends to decrease the boundary layer thickness and thus enhances the heat and mass transfer rates between the fluid and the wall. Moreover, the heat and mass transfer rates of the cylinder with slender orientation are higher than those of the cylinder with blunt orientation.

Key-Words: - Heat and mass transfer, Permeable, Natural convection, Porous medium, Elliptic cylinder, Cubic Spline collocation method, Coordinate transformation

1 Introduction

Coupled heat and mass transfer driven by combined thermal and solutal buoyancy forces in a fluid-saturated porous medium is of great importance in geophysical, geothermal and industrial applications, such as the extraction of geothermal energy, the dispersion of chemical contaminants through water-saturated soil and the migration of moisture through air contained in fibrous insulations.

Bejan and Khair [1] used Darcy's law to study the features of natural convection boundary layer flow driven by temperature and concentration gradients. Lai and Kulacki [2] studied the natural convection boundary layer along a vertical surface with constant heat and mass flux including the effect of wall injection. Yih [3] studied the heat and mass transfer characteristics in natural convection flow over a truncated cone subjected to variable wall temperature and concentration or variable heat and mass flux embedded in porous media. Cheng [4] uses integral approach to study the magnetic effects on heat and mass transfer by natural convection from a vertical plate in a fluid-saturated porous medium.

Similarity solutions for natural convection heat transfer on a horizontal cylinder in a saturated porous medium have been presented by Merkin [5]. Fand et al. [6] examined experimentally the heat transfer characteristics by natural convection from a horizontal cylinder embedded in porous media. Yücel [7] studied the heat and mass transfer about a vertical cylinder with constant wall temperature and concentration in a porous medium. Yih [8] examined the heat and mass transfer by natural convection from a permeable horizontal cylinder in a porous medium with constant wall temperature and concentration. Merkin [9] studied the natural convection boundary layer flow on cylinders of elliptic cross section in a porous medium. Pop et al. [10] examined the natural convection heat transfer about cylinders of elliptic cross section in a porous medium.

Motivated by the works above, this article applied the coordinate transformation and the cubic spline collocation method to analyze the heat and mass transfer by natural convection along a permeable horizontal cylinder of elliptic cross section embedded in fluid saturated porous media with constant wall temperature and concentration. The results obtained herein are compared with the similarity solutions for horizontal cylinders obtained by Merkin [5] and by Yih [8] to check the accuracy. The influence of the transpiration parameter and the eccentricity on the heat and mass transfer characteristics near a permeable horizontal cylinder of elliptic cross section in a fluid-saturated porous

medium is examined when the major axis is horizontal (blunt orientation) and vertical (slender orientation).

2 Problem Formulation

Consider the effect of transpiration on the combined heat and mass transfer by free convection near a buried horizontal cylinder of elliptic cross section with blunt orientation embedded in a homogeneous fluid-saturated porous medium, as shown in Fig. 1, where *a* is the length of semi-major axis and *b* is the length of semi-minor axis for the elliptical cylinder. In this figure, *A* represents the angle made by the outward normal from the cylinder with the downward vertical and *B* is the eccentric angle. It should be noted that for cylinders of elliptic cross section there are two orientations to consider: the orientation is blunt when the major axis is horizontal, as shown in Fig. 1, and the orientation is slender when the major axis is vertical.

The surface of the cylinder is held at a constant temperature T_w which is higher than the ambient porous medium temperature T_∞. In addition, the concentration of a certain constituent in the solution that saturates the porous medium varies from C_w on the fluid side of the surface of the cylinder to C_∞ sufficiently far from the surface of the cylinder. The transpiration velocity is uniform. The fluid properties are assumed to be constant except for density variations in the buoyancy force term.

With introducing the boundary layer and Boussinesq approximations, the equations governing the steady-state conservation of mass, momentum, energy and constituent for Darcian flow through a homogeneous porous medium near the surface of the horizontal cylinder of elliptic cross section can be written in two-dimensional Cartesian coordinates (x, y) as [10]

$$\frac{\partial u}{\partial x}+\frac{\partial v}{\partial y}=0 \tag{1}$$

$$u=\frac{K\sin A}{\mu}\left[\rho g\beta_t\left(T-T_\infty\right)+\rho g\beta_c\left(C-C_\infty\right)\right] \tag{2}$$

$$u\frac{\partial T}{\partial x}+v\frac{\partial T}{\partial y}=\alpha\frac{\partial^2 T}{\partial y^2} \tag{3}$$

$$u\frac{\partial C}{\partial x}+v\frac{\partial C}{\partial y}=D\frac{\partial^2 C}{\partial y^2} \tag{4}$$

The appropriate boundary conditions are:

$$v=V_w,\ T=T_w,\ C=C_w \text{ on } y=0 \tag{5}$$

$$u=0,\ T=T_\infty,\ C=C_\infty \text{ as } y\to\infty \tag{6}$$

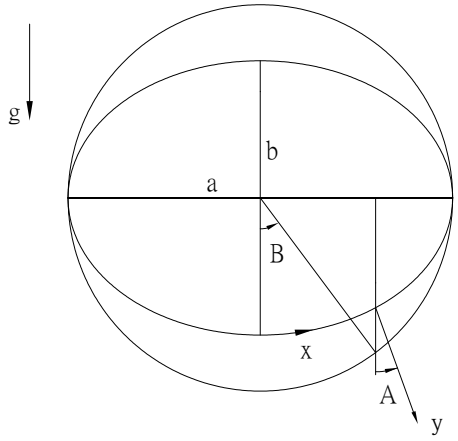

Fig. 1. Physical model and coordinates for an elliptic cylinder of blunt orientation.

Here *u* and *v* are the volume-averaged velocity components in the x-direction and y-direction, respectively. T and C are the volume-averaged temperature and concentration, respectively. Property μ is the dynamic viscosity of the fluid, K is the permeability of the porous medium, and ρ is the fluid density. Furthermore, α and D are the equivalent thermal and mass diffusivity of the saturated porous medium, respectively. β_t and β_c are the coefficients for thermal expansion and for concentration expansion of the saturated porous medium, respectively, and g is the gravitational acceleration. V_w is the uniform transpiration velocity.

After introducing the stream function $\overline{\psi}$ to satisfy the relations: $u=\partial\overline{\psi}/\partial y$ and $v=-\partial\overline{\psi}/\partial x$, we then define the nondimensional variables: $\xi=x/a$, $\eta=\left(y/a\right)Ra^{1/2}$, $\psi=\overline{\psi}/\left(\alpha Ra^{1/2}\right)$, $\theta=\left(T-T_\infty\right)/\left(T_w-T_\infty\right)$, $\phi=\left(C-C_\infty\right)/\left(C_w-C_\infty\right)$. Equations (1)-(6) become the following equations:

$$\frac{\partial\psi}{\partial\eta}=\left(\theta+NC\right)\sin A \tag{7}$$

$$\frac{\partial\psi}{\partial\eta}\frac{\partial\theta}{\partial\xi}-\frac{\partial\psi}{\partial\xi}\frac{\partial\theta}{\partial\eta}=\frac{\partial^2\theta}{\partial\eta^2} \tag{8}$$

$$\frac{\partial\psi}{\partial\eta}\frac{\partial\phi}{\partial\xi}-\frac{\partial\psi}{\partial\xi}\frac{\partial\phi}{\partial\eta}=\frac{1}{Le}\frac{\partial^2\phi}{\partial\eta^2} \tag{9}$$

The associated boundary conditions are

$$\frac{\partial\psi}{\partial\xi}=-\frac{V_w a}{\alpha Ra^{1/2}},\ \theta=1,\ \phi=1 \text{ on } \eta=0 \tag{10}$$

$$\frac{\partial\psi}{\partial\eta}=0,\ \theta=0,\ \phi=0 \text{ as } \eta\to\infty \tag{11}$$

In the above equations, $Ra = K\beta_t ga(T_w - T_\infty)/(\alpha\nu)$ is the Darcy-Rayleigh number, $Le = \alpha/D$ is the Lewis number and $N = \beta_c(C_w - C_\infty)/[\beta_t(T_w - T_\infty)]$ is the buoyancy ratio.

A further transformation is needed for bodies with rounded lower ends because $\sin A/\xi$ approaches a constant value as ξ approaches zero [10]. The new nondimensional variable is defined as

$$f(\xi,\eta) = \xi^{-1}\psi \tag{12}$$

Substituting Eq. (12) into Eqs. (7)-(9), we obtain the following boundary-layer governing equations:

$$f' = \frac{\sin A}{\xi}(\theta + N\phi) \tag{13}$$

$$\theta'' + f\theta' = \xi\left(f'\frac{\partial\theta}{\partial\xi} - \theta'\frac{\partial f}{\partial\xi}\right) \tag{14}$$

$$\frac{1}{Le}\phi'' + f\phi' = \xi\left(f'\frac{\partial\phi}{\partial\xi} - \phi'\frac{\partial f}{\partial\xi}\right) \tag{15}$$

The boundary conditions are

$$f = f_w,\ \theta = 1,\ \phi = 1 \text{ on } \eta = 0 \tag{16}$$

$$f' = 0,\ \theta = 0,\ \phi = 0 \text{ as } \eta \to \infty \tag{17}$$

In terms of the new variables, the Darcian velocities in x- and y- directions can be expressed as

$$u = \frac{\alpha\xi Ra}{a} f' \tag{18}$$

$$v = -\frac{\alpha Ra^{1/2}}{a}\left(f + \xi\frac{\partial f}{\partial\xi}\right) \tag{19}$$

Here primes denotes partial derivation with respect to η. As $b/a = 1$, $N = 0$ and $f_w = 0$, Eqs. (13)-(14) become the equations for the Darcy natural convection heat transfer near a horizontal circular cylinder in a fluid-saturated porous medium presented by Merkin [5]. $f_w = -(V_w a)/\alpha Ra^{1/2}$ is the transpiration parameter. Note that $f_w < 0$ when $V_w > 0$ (the case of blowing), and $f_w > 0$ when $V_w < 0$ (the case of suction).

Here ξ and $\sin A$ can be given in terms of the eccentric angle B by the relations:

(1) For blunt orientation:

$$\xi = \int_0^B \left(1 - e^2 \sin^2\gamma\right)^{1/2} d\gamma \tag{20}$$

$$\sin A = \frac{b}{a}\frac{\sin B}{\left(1 - e^2 \sin^2 B\right)^{1/2}} \tag{21}$$

(2) For slender orientation:

$$\xi = \int_0^B \left(1 - e^2 \cos^2\gamma\right)^{1/2} d\gamma \tag{22}$$

Table 1. The value of $F_{i,j}$, $G_{i,j}$, and $S_{i,j}$.

θ	$F_{i,j}$	$\theta^n_{i,j} + \Delta\tau\left[-\xi_i l_f^n \left(\frac{\partial\theta}{\partial\xi}\right)^n_{i,j}\right]$
	$G_{i,j}$	$\Delta\tau\left[f^n_{i,j} + \xi_i\left(\frac{\partial f}{\partial\xi}\right)^{n+1}_{i,j}\right]$
	$S_{i,j}$	$\Delta\tau$
ϕ	$F_{i,j}$	$\phi^n_{i,j} + \Delta\tau\left[-\xi_i l_f^{n+1}\left(\frac{\partial\phi}{\partial\xi}\right)^n_{i,j}\right]$
	$G_{i,j}$	$\Delta\tau\left[f^n_{i,j} + \xi_i\left(\frac{\partial f}{\partial\xi}\right)^n_{i,j}\right]$
	$S_{i,j}$	$\frac{\Delta\tau}{Le}$

Table 2. Comparison of values of $Nu/\sqrt{Ra}$ for $N = 0$ and $b/a = 1$ between the present results with the solutions reported by Merkin [5] and Yih [8].

ξ	Merkin [5]	Yih [8]	Present results
0	0.6276	0.6276	0.6276
0.2	0.6245	0.6245	0.6245
0.6	0.5996	0.5996	0.5997
1.0	0.5508	0.5508	0.5510
1.4	0.4800	0.4800	0.4804
1.8	0.3901	0.3899	0.3904
2.2	0.2847	0.2843	0.2849
2.6	0.1679	0.1677	0.1680
3.0	0.0444	0.0446	0.0444

$$\sin A = \frac{\sin B}{\left(1 - e^2 \cos^2 B\right)^{1/2}} \tag{23}$$

where e denotes the eccentricity expressed as $e = \left(1 - b^2/a^2\right)^{1/2}$ and b/a is the aspect ratio of the elliptic cylinder. When ξ approaches zero, as shown In Eqs. (20)-(23), the value of $\sin A/\xi$ approaches the aspect ratio b/a for the elliptic cylinder with blunt orientation while the value of $\sin A/\xi$

approaches the value of a^2/b^2 for the elliptic cylinder with slender orientation.

The local Nusselt number can be written as

$$\frac{Nu}{Ra^{1/2}} = -\theta'(\xi,0) \tag{24}$$

The local Sherwood number can be given by

$$\frac{Sh}{Ra^{1/2}} = -\phi'(\xi,0) \tag{25}$$

In Eqs. (24)-(25), $Nu = ha/k$ and $Sh = ja/D$ where h and j are the local heat transfer coefficient and the local mass transfer coefficient, respectively.

The average Nusselt number for the elliptic cylinder can be derived as:

(1) For blunt orientation

$$\frac{Nu_m}{Ra^{1/2}} = -\frac{\int_0^{\pi} \theta'(\xi,0)\left(1-e^2\sin^2\gamma\right)^{1/2} d\gamma}{\int_0^{\pi}\left(1-e^2\sin^2\gamma\right)^{1/2} d\gamma} \tag{26}$$

(2) For slender orientation

$$\frac{Nu_m}{Ra^{1/2}} = -\frac{\int_0^{\pi} \theta'(\xi,0)\left(1-e^2\cos^2\gamma\right)^{1/2} d\gamma}{\int_0^{\pi}\left(1-e^2\cos^2\gamma\right)^{1/2} d\gamma} \tag{27}$$

The average Sherwood number for the elliptic cylinder can be given by:

(1) For blunt orientation

$$\frac{Sh_m}{Ra^{1/2}} = -\frac{\int_0^{\pi} \phi'(\xi,0)\left(1-e^2\sin^2\gamma\right)^{1/2} d\gamma}{\int_0^{\pi}\left(1-e^2\sin^2\gamma\right)^{1/2} d\gamma} \tag{28}$$

(2) For slender orientation

$$\frac{Sh_m}{Ra^{1/2}} = -\frac{\int_0^{\pi} \phi'(\xi,0)\left(1-e^2\cos^2\gamma\right)^{1/2} d\gamma}{\int_0^{\pi}\left(1-e^2\cos^2\gamma\right)^{1/2} d\gamma} \tag{29}$$

Note that $Nu_m = h_m a/k$ and $Sh_m = j_m a/D$ where h_m and j_m are the average heat transfer coefficient and the average mass transfer coefficient for the elliptic cylinder, respectively.

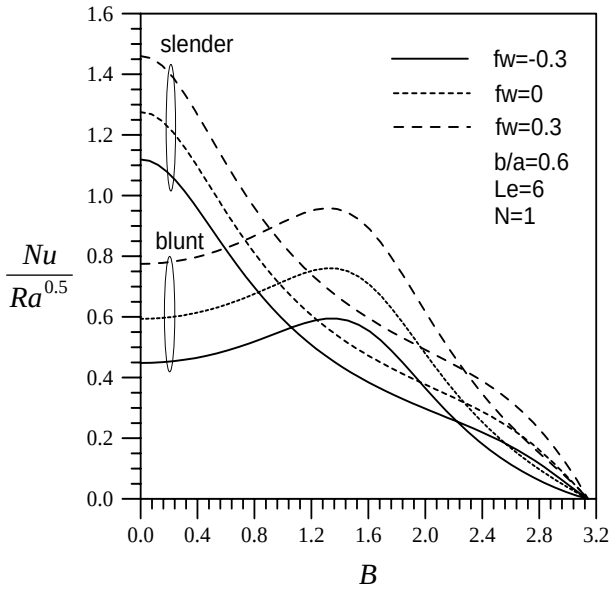

Fig. 2. Effects of transpiration parameter on the local Nusselt number.

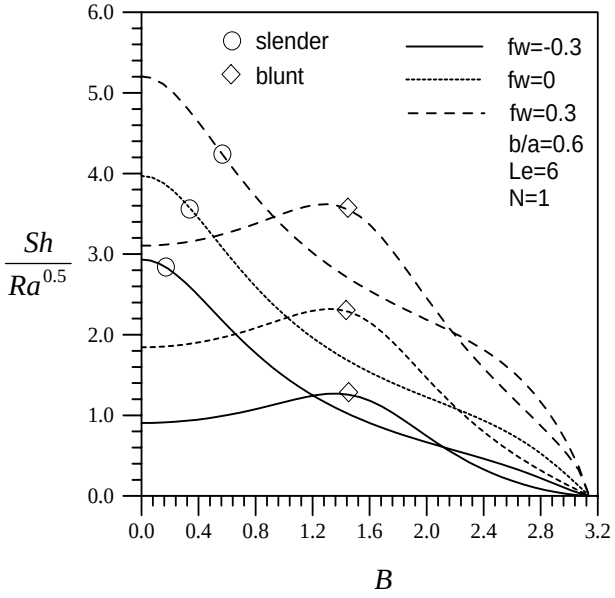

Fig. 3. Effects of transpiration parameter on the local Sherwood number.

3 Problem Solution

The governing differential equations, Eqs. (14) and (15), and the appropriate boundary conditions, Eqs. (16) and (17), can be solved by the cubic spline collocation method [11, 12]. The Simpson's rule for variable grids is used to calculate the value of f at every position from Eq. (13) and boundary conditions (16) and (17). Variable grids with 200 grid points are used in the η direction. The minimum step size is 0.01. The value of the edge of the boundary layer η_∞ is about 12. Moreover, a grid with 150 grid points is used in the ξ direction. At every grid point, the iteration process continues until the convergence criterion for all the variables, 10^{-6}, is achieved. The present calculation for Eqs. (13)-(17) can be performed from the bottom up to the top of the elliptic cylinder without encountering a singularity.

Here by using the cubic spline collocation method [11, 12], Eqs. (14) and (15) can be discretized by using the false transient technique, as

$$\frac{\theta_{i,j}^{n+1}-\theta_{i,j}^{n}}{\Delta\tau}+\xi_i l_f^n\left(\frac{\partial\theta}{\partial\xi}\right)_{i,j}^{n}-\xi_i l_\theta^{n+1}\left(\frac{\partial f}{\partial\xi}\right)_{i,j}^{n}$$
$$=L_\theta^{n+1}+f_{i,j}^{n}l_\theta^{n+1} \quad (30)$$

$$\frac{\phi_{i,j}^{n+1}-\phi_{i,j}^{n}}{\Delta\tau}+\xi_i l_f^n\left(\frac{\partial\phi}{\partial\xi}\right)_{i,j}^{n}-\xi_i l_\phi^{n+1}\left(\frac{\partial f}{\partial\xi}\right)_{i,j}^{n}$$
$$=\frac{L_\phi^{n+1}}{Le}+f_{i,j}^{n}l_\phi^{n+1} \quad (31)$$

where

$$\Delta\xi=\xi_i-\xi_{i-1},\ \Delta\eta=\eta_i-\eta_{i-1}$$

$$\left(\frac{\partial\vartheta}{\partial\xi}\right)_{i,j}=\frac{\vartheta_{i,j}-\vartheta_{i,j-1}}{\Delta\xi_i}\ \text{for}\ i=1$$

$$\left(\frac{\partial\vartheta}{\partial\xi}\right)_{i,j}=\frac{-3\vartheta_{i,j}+4\vartheta_{i,j-1}-\vartheta_{i,j-2}}{2\Delta\xi_i}\ \text{for}\ i\geq 2$$

$$l_\phi=\frac{\partial\vartheta}{\partial\eta},\ L_\phi=\frac{\partial^2\vartheta}{\partial\eta^2} \quad (32)$$

Note that ϑ refers to θ and ϕ, and the quantity $\Delta\tau=\tau^{n+1}-\tau^{n}$ represents the false time step.

After some arrangement, Eqs. (30) and (31) can be written in the following spline approximation form:

$$\vartheta_{i,j}^{n+1}=F_{i,j}+G_{i,j}l_{\vartheta_{i,j}}^{n+1}+S_{i,j}L_{\vartheta_{i,j}}^{n+1} \quad (33)$$

The quantities *F*, *G*, and *S* are known coefficients evaluated at previous time steps (Table 1). By using the cubic spline relations [11, 12], Eq. (33) may be written in the following tridiagonal form as

$$A_{i,j}\vartheta_{i,j-1}+B_{i,j}\vartheta_{i,j}+C_{i,j}\vartheta_{i,j+1}=D_{i,j} \quad (34)$$

Here Eq. (34) can be easily solved by using the Thomas algorithm.

In order to check the accuracy of the present method, the local Nusselt number $Nu/Ra^{0.5}$ for $b/a=1$ and $N=0$ obtained in the current study under Darcian assumptions for a horizontal circular cylinder are compared with the solutions reported by Merkin [5] and Yih [8]. As shown in Table 2, the present results are found to be in excellent agreement with the results of Merkin [5] and Yih [8].

Figs. 2 and 3 plot the variation of the local Nusselt number $Nu/Ra^{0.5}$ and the local Sherwood number Sherwood number $Sh/Ra^{0.5}$ as functions of the eccentric angle *B* of the elliptical cylinder for various transpiration parameters (f_w = -0.3, 0, 0.3), *N*=1, *Le*=6 and *b/a*=0.6. For the elliptical cylinder with blunt orientation, the local Nusselt number and the local Sherwood number first increase with distance from the stagnation point, reach a maximum,

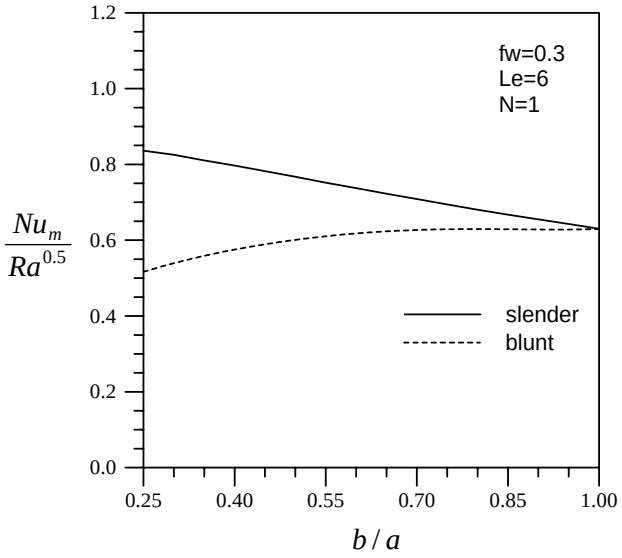

Fig. 4. Effects of aspect ratio on the average Nusselt number.

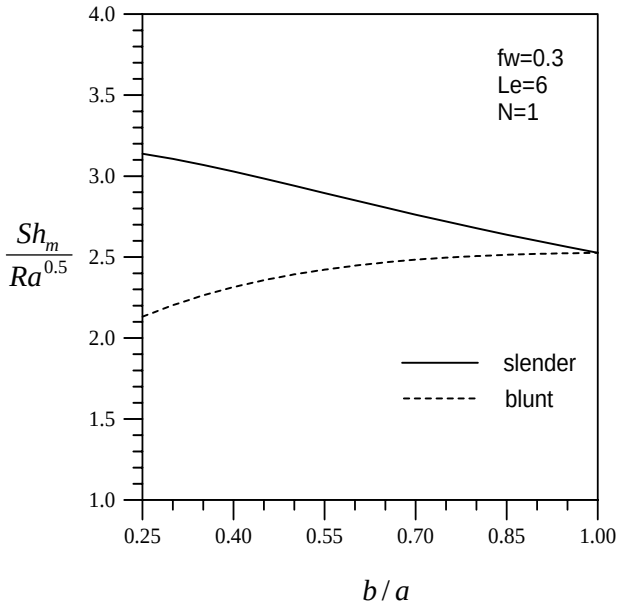

Fig. 5. Effects of aspect ratio on the average Sherwood number.

and then decrease to zero at the top of the elliptical cylinder. For an elliptical cylinder with slender orientation, the local Nusselt number and the local Sherwood number decrease monotonically from the lower end of the cylinder to the upper end of the cylinder; that is due to the increase in boundary layer thickness.

Comparing the curves in Figs. 2 and 3, we can deduce that increasing the transpiration parameter tends to decrease the boundary layer thickness and thus increases the heat and mass transfer rates between the fluid and the wall. The results show that

the use of blowing ($f_w < 0$ and $V_w > 0$) tends to decrease the heat and mass transfer rate while the use of suction ($f_w > 0$ and $V_w < 0$) increases the heat and mass transfer rate.

Figs. 4 and 5 show the average Nusselt number $Nu_m / Ra^{0.5}$ and the average Sherwood number $Sh_m / Ra^{0.5}$ as a function of the aspect ratio *b/a* for $f_w = 0.3$, *Le*=6 and *N*=1. The average Nusselt number and the average Sherwood number of the elliptic cylinder with slender orientation are higher than those of the elliptical cylinder with blunt orientation for any aspect ratio *b/a* smaller than one. When the aspect ratio *b/a* is increased (i.e., the eccentricity is decreased), the average Nusselt number and the average Sherwood number for the elliptic cylinder of slender orientation tend to decrease while those for the elliptic cylinder of blunt orientation tend to increase, and finally the average Nusselt number and the average Sherwood number of slender orientation equal to those of blunt orientation when the aspect ratio *b/a* equals to one. Therefore, the elliptic cylinders of slender orientation are found to be superior to the elliptic cylinders of blunt orientation from the viewpoint of the heat and mass transfer rates in fluid-saturated porous media.

4 Conclusion

The coupled heat and mass transfer by natural convection of a permeable horizontal cylinder with elliptic cross section has been studied. Here a coordinate transformation is employed to transform the governing equations into nondimensional nonsimilar boundary layer equations. The obtained boundary layer equations are then solved by the cubic spline collocation method. The effects of the transpiration parameter and the aspect ratio on the Nusselt and Sherwood numbers for the permeable elliptical cylinders of blunt and slender orientations have been studied. The results show that increasing the transpiration parameter tends to decrease the boundary layer thickness and thus enhances the heat and mass transfer rates between the fluid and the wall. Moreover, the heat and mass transfer rates of the cylinder with slender orientation are higher than those of the cylinder with blunt orientation.

Acknowledements

This work was supported by National Science Council of Republic of China under the grant no. NSC 94-2212-E-218-016.

References:

[1] A. Bejan, K.R. Khair, Heat and Mass Transfer by Natural Convection in a Porous Medium, *International Journal of Heat and Mass Transfer*, Vol. 28, 1985, pp. 909-918.

[2] F.C. Lai, F.A. Kulacki, Coupled Heat and Mass Transfer by Natural Convection from Vertical Surfaces in Porous Media," *International Journal of Heat and Mass Transfer*, Vol. 34, 1991, pp. 1189-1191.

[3] K.A. Yih, Coupled Heat and Mass Transfer by Free Convection over a Truncated Cone in Porous Media: VWT/VWC or VHF/VMF, *Acta Mechanica*, Vol. 137, 1999, pp. 83-97.

[4] C.Y. Cheng, Effect of a Magnetic Field on Heat and Mass Transfer by Natural Convection from Vertical Surfaces in Porous Media-an Integral Approach, *International Communications in Heat and Mass Transfer*, Vol. 26, 1999, pp. 935-943.

[5] J.H. Merkin, Free Convection Boundary Layers on Axi-Symmetric and Two-Dimensional Bodies of Arbitrary Shape in a Saturated Porous Medium, *International Journal of Heat and Mass Transfer*, Vol. 22, 1979, pp. 1461-1462.

[6] R.M. Fand, T.E. Steinberger, P. Cheng, Natural Convection Heat Transfer from a Horizontal Cylinder Embedded in a Porous Medium, *International Journal of Heat and Mass Transfer*, Vol. 29, 1986, pp. 119-133.

[7] A. Yücel, Natural Convection Heat and Mass Transfer along a Vertical Cylinder in a Porous Medium, *International Communications in Heat and Mass Transfer*, Vol. 33, 1990, pp. 2265-2274.

[8] K.A. Yih, Coupled Heat and Mass Transfer by Natural Convection Adjacent to a Permeable Horizontal Cylinder in a Saturated Porous Medium, *International Communications in Heat and Mass Transfer*, Vol. 26, 1999, pp. 431-440.

[9] J.H. Merkin, Free Convection Boundary Layers on Cylinders of Elliptic Cross Section, *Journal of Heat Transfer*, Vol. 99, 1977, pp. 453-457.

[10] I. Pop, M. Kumari, G. Nath, Free Convection about Cylinders of Elliptic Cross Section Embedded in a Porous Medium, *International Journal of Engineering Science*, Vol. 30, 1992, pp. 35-45.

[11] S.G. Rubin, R.A. Graves, Viscous Flow Solution with a Cubic Spline Approximation, *Computers and Fluids*, Vol. 3, 1975, pp. 1-36.

[12] P. Wang, R. Kahawita, Numerical Integration of Partial Differential Equations Using Cubic Spline, *International Journal of Computer Mathematics*, Vol. 13, 1983, pp. 271-286.